

Efficient Long-Context Modeling in Diffusion Language Models via Block Approximate Sparse Attention

Wenhu Zhang¹ Yiming Wu² Huanyu Wang³ Yaoyang Liu¹ Huanzhang Dou³
Senqiao Yang⁴ Sitong Wu⁴ Hanbin Zhao³ Jiaya Jia¹✉

¹The Hong Kong University of Science and Technology ²The University of Hong Kong
³Zhejiang University ⁴The Chinese University of Hong Kong

Abstract

*Diffusion Language Models (DLMs) enable globally coherent, bidirectional, and controllable text generation, offering advantages over traditional autoregressive LLMs, while scaling to ultra-long sequences remains costly. Many existing block-sparse attention methods select blocks by fixed sampling patterns over the high-resolution attention space, e.g. tail-regions or anti-diagonal stripes. Such prior-driven sampling can miss salient tokens and introduce instability under distribution shifts. In this paper, we propose the Block Approximate Sparse Attention framework (BA-Att) with block-wise pre-downsampled operation, which identifies informative regions within a compact downsampled spaces, avoiding reliance on brittle positional priors. To analyze its theoretical behavior, we define an oracle post-downsample attention map and formalize the approximation error between pre- and post-downsample schemes. Based on this insight, we introduce a lightweight norm-sorting module and a covariance-compensated correction that approximates full covariance using diagonal QK variances, reducing large computational complexity. Extensive experiments show that our operator achieves up to **6.95× acceleration** over FlashAttention in attention computation, and maintains **near full-attention performance** at 50% sparsity across language models, multi-modal language models, and video generation models, demonstrating strong efficiency and generalization.*

1. Introduction

Diffusion Language Models (DLMs), *a.k.a.* Masked Diffusion Models, are rapidly emerging as a non-autoregressive alternative to traditional autoregressive LLMs. Compared

to models such as GPT or LLaMA, DLMs offer several potential advantages in generation dynamics, contextual understanding, and controllability. Specifically, DLMs formulate text generation as a gradual denoising process that iteratively refines a noisy linguistic representation into a clean sentence. This paradigm enables globally coherent generation with improved long-range and bidirectional context modeling, positioning DLMs as a key direction for next-generation generative language modeling.

However, scaling DLMs to ultra-long contexts poses significant computational challenges. The introduction of sparse attention has been a key step toward improving efficiency, allowing models to focus computation on structurally or semantically salient regions. Two typical routines are proposed to solve this problem. The first is learning gating modules to predict importance. *e.g.*, SeerAttention [13] proposes a mechanism to learn and operate the downsampled block spaces. However, these methods require additional training, limiting real world deployment. Second, motivated by empirical observations, a series of methods attempt to design training-free strategies, such as the A-Shape pattern from StreamingLLM [47], the Vertical-Slash mechanisms from MInference [21], query-specific patterns in FlexPrefill [23], and the Antidiagonal scoring strategy from XAttention [48]. However, most training-free sparse attention relying on fixed positional priors would miss salient tokens. This raises a fundamental question: *Can we design a **training-free** sparse attention method that operates effectively in the **downsampled attention space**, while preserving both efficiency and robustness without any fine-tuning?*

In this paper, we propose Block Approximate Sparse Attention (**BA-Att**), a block-wise downsampling framework. Our method introduces a pre-downsampling stage that evaluates the information quality of each block directly in the downsampled attention space, thereby avoiding reliance on heuristic positional priors. To ground the method in theory, we analyze the ideal upper bound and formalize

Code will be publicly available at: <https://github.com/JIA-Lab-research/Block-Approximate-Sparse-Attention>.

✉ Corresponding Author.

Table 1. Comparison of sparse attention selection strategies. **Pattern-Agnostic**: no reliance on fixed structural priors (e.g., sink, vertical, diagonal). **Downsampled Search**: pattern selection is performed in a downsampled token or block space. **Search Space Coverage**: fraction of the full $Q \times K$ attention matrix examined during selection. **Search Complexity**: asymptotic cost of the selection stage w.r.t. sequence length L , with block size B (typically 64 or 128 tokens) and stride s (typically 8 or 16).

Method	Pattern-Agnostic	Training-Free	Search Space Coverage	Search Complexity
MInference [21]	✗	✓	< 5%	$O(LB)$
FlexPrefill [23]	✗	✓	< 5%	$O(LB)$
XAttention [48]	✗	✓	12.5%	$O(L^2/s)$
SeerAttention [13]	✓	✗	100%	$O((L/B)^2)$
Ours	✓	✓	100%	$O((L/B)^2)$

the approximation error between the pre-downsample and post-downsample schemes, providing a principled characterization of the efficiency–fidelity trade-off inherent in block-sparse attention. This formulation further allows us to define an oracle attention map induced by the post-downsampling computation. From the high-level comparisons in Table 1, BA-Att achieves full coverage in a downsampled space without any post-training, while others either depend on fixed structural assumptions or suffer from limited search coverage.

Building upon the theoretical analysis, we show that the approximation error grows with the intra-block norm range of QK pairs; in other words, large norm disparities within a block lead to dispersed attention patterns and degrade performance. To address this issue, we introduce a lightweight norm-sorting module with complexity $O(L \times D)$, which reorders tokens by their norm magnitude to reduce approximation difficulty and cluster high-activation regions. Based on the resulting error formulation, we further derive a covariance-compensated correction scheme that improves accuracy without sacrificing efficiency. Specifically, we approximate the full covariance term using the diagonal combination of QK variances, reducing the overall attention complexity from $O(L \times D^2)$ to $O(L \times D)$.

We conduct extensive experiments to validate the efficiency and effectiveness. Under a **sequence length of 128K**, our method achieves a 6.95× speedup over Flash-Attention. When integrated into **diverse DLMs**, our method consistently matches the performance of full attention at 50% sparsity. **In video generation**, our method surpasses SOTA video generation methods, clearly demonstrating the superior fidelity–efficiency trade-off. The contributions are summarized as follows:

- **Pre-downsampled Block-Sparse Attention.** We propose a Block Approximate Sparse Attention framework that evaluates the block quality in the downsampled attention space, without any finetuning, and improving scalability to ultra-long sequences.
- **Norm-Sorting and Covariance Compensation.** Based on our theoretical analysis, we mitigate the approxima-

tion errors via a lightweight norm-sorting module and a covariance-compensated correction, achieving more accurate attention patterns.

- **Empirical Validation and Scalability.** As a result, our BA-Att achieves up to 6.95× speedup over FlashAttention and maintains almost full-attention performance at about 50% sparsity across ultra-long sequence tasks.

2. Preliminaries

Scaled Dot-Product Attention As a fundamental component of modern large language models, scaled dot-product attention (SDPA) aggregates contextual information through a weighted summation of value vectors, proving highly effective for modeling long-range dependencies. Let Q and K be the RoPE-enhanced queries and keys, and V be the values, the attention mechanism is computed as

$$A = \text{softmax}\left(\frac{QK^\top}{\sqrt{d}}\right), \quad (1)$$

where A_{ij} denotes the attention weight from query position i to key position j . This formulation allows queries directly attend to every KV pair, enabling long-range interactions at the cost of quadratic complexity $O(L^2)$.

Block-Sparse Attention To reduce the $O(L^2)$ overhead, Flash-Attention [8] reorganizes attention into block-wise computations that leverage fast on-chip memory. Let the block size be B , and the numbers of query and key blocks as $N_q = \frac{L_q}{B}$, $N_k = \frac{L_k}{B}$, where L_q and L_k are length of query and key. Building on this design, subsequent works further improve the computational efficiency by introducing block-sparse patterns that prune interactions at the block level.

In block-sparse attention, we only compute logits of selected blocks. The block-level binary mask is denoted as $M \in \{0, 1\}^{N_q \times N_k}$. For convenience, we use lower-case i, j for token indices, and g_q, g_k for block indices. An item in the block mask M indicates a block pair (g_q, g_k) in the obtained sparse attention map. For each query block Q_{g_q} , the computation for the corresponding output O_{g_q} is associated with a few number of key-value blocks (*i.e.* K_{g_k}, V_{g_k}),

which are selected by $M_{g_q, g_k} = 1$. Thus, specifying a block-sparse attention pattern is to construct a block mask M over $N_q \times N_k$.

3. Method

As is shown in Fig. 1, we introduce a training-free *block-sparse attention framework* including three core components: a downsampled block-sparse formulation together with an oracle block mask, a norm-based ranking that reshapes blocks to be more homogeneous, and a covariance-based compensation that recovers performance loss.

3.1. Pre-downsampled Attention Map

We construct a downsampled block-sparse baseline to establish a reference formulation. First, we employ mean pooling to obtain representative block embeddings \bar{Q}_{g_q} and \bar{K}_{g_k} , where g_q, g_k are indices of the query and key blocks. Based on the downsampled representations, we compute block-level logits ℓ_{g_q, g_k} and the corresponding query-block distribution m_{g_q, g_k} as :

$$\begin{aligned} \ell_{g_q, g_k} &= (\bar{Q}_{g_q} \cdot \bar{K}_{g_k}) / \sqrt{d}, \\ m_{g_q, g_k} &= \text{softmax}(\ell) = \exp(\ell_{g_q, g_k}) / \sum_{g'_k=1}^{N_k} \exp(\ell_{g_q, g'_k}), \end{aligned} \quad (2)$$

where d denotes the feature dimension. The block-sparse attention mask M is subsequently constructed according to the block distribution m_{g_q, g_k} under different computational budgets. Attention computation is then confined to the selected block pairs, where we employ efficient FlashAttention-style Triton [39] kernels to perform the final weighted aggregation.

Oracle block distribution. To provide an upper bound for analysis and approximation, we define an oracle block distribution that directly aggregates the token-level attention scores in the high-resolution space. Let A_{ij} denote the attention weight from query token i to key token j within the full attention matrix A from Eq. (1). The oracle block mass for block (g_q, g_k) is

$$\hat{m}_{g_q, g_k} = \frac{1}{|I(g_q)|} \sum_{i \in I(g_q)} \sum_{j \in J(g_k)} A_{ij}, \quad (3)$$

where $I(g_q), J(g_k)$ denotes the index sets belonging to the block. Since computing \hat{m} requires the full dense attention map, we use it as the target and an empirical reference for evaluating the fidelity of our approximate block distributions.

3.2. Downsampling Deviation Analysis

Our objective is to make the downsampled attention distribution m as close as the oracle distribution \hat{m} . However, di-

rectly analyzing their divergence in the softmax space is analytically intractable due to the normalization coupling and exponential nonlinearity in softmax. Following prior analyses of approximation errors in attention mechanisms [7, 9], we instead examine the deviation at the *pre-softmax logit* level as a surrogate.

The softmax operator is known to be *Lipschitz continuous* under the ℓ_∞ norm and smooth under ℓ_2 perturbations [3]. Consequently, a small perturbation in the logits yields a bounded change in the resulting attention distribution. Formally, for any two logit matrices ℓ and $\hat{\ell}$, we have

$$\|\text{softmax}(\ell) - \text{softmax}(\hat{\ell})\|_1 \leq C \|\ell - \hat{\ell}\|_\infty, \quad (4)$$

where C is a bounded constant depending on the temperature. Let $\hat{\ell}_{ij} = (Q_i \cdot K_j) / \sqrt{d}$ represents the pre-softmax token-level logit. This property implies that controlling the logit-level deviation $|\hat{\ell}_{ij} - \ell_{g_q, g_k}|$ provides a valid proxy for bounding the difference between m and \hat{m} . Therefore, we focus our analysis on the geometric factors that govern this logit deviation, which further motivates the proposed norm-sorting and covariance-compensated designs.

We rewrite $Q_i = \bar{Q}_{g_q} + \delta Q_i$, $K_j = \bar{K}_{g_k} + \delta K_j$. Then, the deviation between the token-level logit $\hat{\ell}_{ij}$ and its corresponding block-level logit ℓ_{g_q, g_k} in Eq. (2), is written as:

$$\hat{\ell}_{ij} - \ell_{g_q, g_k} = \frac{1}{\sqrt{d}} (\delta Q_i \cdot \bar{K}_{g_k} + \bar{Q}_{g_q} \cdot \delta K_j + \delta Q_i \cdot \delta K_j). \quad (5)$$

By applying Cauchy-Schwarz, we obtain a formulation as :

$$\begin{aligned} |\delta Q_i \cdot \bar{K}_{g_k}| &\leq R_{g_q}^Q M_{g_k}^K, \\ |\bar{Q}_{g_q} \cdot \delta K_j| &\leq M_{g_q}^Q R_{g_k}^K, \\ |\delta Q_i \cdot \delta K_j| &\leq R_{g_q}^Q R_{g_k}^K. \end{aligned} \quad (6)$$

In this way, we define several block-wise norm metrics as :

$$\begin{aligned} R_{g_q}^Q &= \max_{i \in I(g_q)} \|Q_i - \bar{Q}_{g_q}\|_2, & M_{g_q}^Q &= \max_{i \in I(g_q)} \|Q_i\|_2, \\ R_{g_k}^K &= \max_{j \in J(g_k)} \|K_j - \bar{K}_{g_k}\|_2, & M_{g_k}^K &= \max_{j \in J(g_k)} \|K_j\|_2, \end{aligned} \quad (7)$$

where $R_{g_q}^Q$ and $R_{g_k}^K$ are *radii* measuring how far tokens deviate from their block means \bar{Q}_{g_q} and \bar{K}_{g_k} , and $M_{g_q}^Q$ and $M_{g_k}^K$ are *max norms*, which capture the scale inside blocks. Then, max norms are combined with upper bounds on the deviation between token-level and block-level logits U_{g_q, g_k} ,

$$\begin{aligned} U_{g_q, g_k} &= \frac{R_{g_q}^Q M_{g_k}^K + M_{g_q}^Q R_{g_k}^K + R_{g_q}^Q R_{g_k}^K}{\sqrt{d}}, \\ |\hat{\ell}_{ij} - \ell_{g_q, g_k}| &\leq U_{g_q, g_k} \quad (\forall i \in I(g_q), j \in J(g_k)). \end{aligned} \quad (8)$$

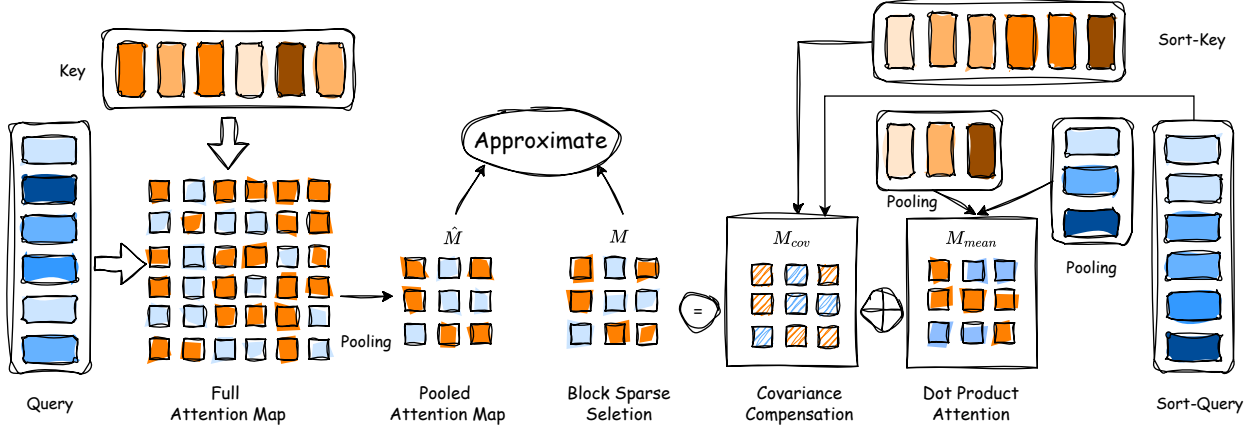
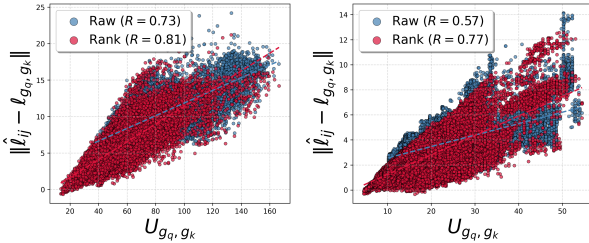


Figure 1. Illustration of our Block Approximate Sparse Attention. Context length $L = 6$ and block size $B = 2$ for simplification in this example. The left part shows the post-downsampled oracle block distribution. The right region details the key steps of our BA-Att, including norm-based QK sort, block-wise pooling, and covariance compensation.



(a) LLaDA-V on VideoMME. (b) UltraLLaDA on Ruler.

Figure 2. Correlation between the Norm-based Metric U_{g_q, g_k} and logit deviation $|\hat{\ell}_{ij} - \ell_{g_q, g_k}|$ across the layers and heads. The blue group represents the vanilla data distribution, and the red group indicates the data after norm-based sorting. The correlation coefficient R of each group shows the linear association.

Interpretation and visualization. In principle, a smaller radii (R^Q, R^K) and moderate max norms (M^Q, M^K) would make blocks homogeneous, thus improving performance. If $R_{g_q}^Q, R_{g_k}^K$ are zeros, standing for perfectly homogeneous blocks, U_{g_q, g_k} would be zero and token-level logits match block logits. As shown in Fig. 2, we visualize the relationship between the theoretical upper bound U_{g_q, g_k} and the observed maximum logit deviation $\max_{i,j} |\hat{\ell}_{ij} - \ell_{g_q, g_k}|$. $R \in [-1, 1]$ is the Pearson correlation coefficient produced by the linear regression model. Blue group represents vanilla data distribution, and $R > 0.5$ indicates that U_{g_q, g_k} is an informative proxy for the true approximation deviation across blocks.

3.3. Norm-Based Ranking

The previous analysis establishes that the deviation between the oracle and pre-downsampled attention distributions is governed by the upper bound U_{g_q, g_k} in Eq. (8), which depends on the intra-block radii (R^Q, R^K) and max norms

(M^Q, M^K). Intuitively, when tokens inside a block exhibit highly uneven norm magnitudes, the resulting query-key interactions become heterogeneous, leading to unstable logits and dispersed attention patterns. Empirical observations in Fig. 2 confirm that blocks with large U_{g_q, g_k} correlate strongly with greater logit deviations and degraded approximation fidelity.

However, under the *training-free* constraint, we cannot rely on learnable gates or additional supervision (as in Seer-Attention [13]) to calibrate these heterogeneous regions. Therefore, a natural question arises: *Can we reshape the block composition itself to reduce U_{g_q, g_k} and make the attention map more homogeneous, without introducing any trainable parameters?*

To this end, we propose a lightweight **norm-based ranking** strategy that reorders tokens by their feature norm before block partitioning. This operation effectively clusters high-activation tokens together, reducing the intra-block variance of QK magnitudes and tightening the theoretical bound U_{g_q, g_k} . Given a key sequence, each key token $j \in \{1, \dots, L_k\}$, define a scalar score,

$$s_j^K = \|K_j\|_2. \quad (9)$$

Let π_k be a permutation that sorts token norms in non-decreasing order

$$s_{\pi_k(1)}^K \leq s_{\pi_k(2)}^K \leq \dots \leq s_{\pi_k(L_k)}^K, \quad (10)$$

and define the permuted query sequence $K'_i = K_{\pi_k(i)}$. Then, we form new query blocks on K' by grouping consecutive indices of size B . We can analogously permute queries using $s_i^Q = \|Q_i\|_2$ to obtain Q' . Under common heavy-tailed activation patterns, sorting by norm and grouping noticeably decreases within-block variance and radii.

Effect on the deviation bound. In practice, norm-based ranking substantially reduces the empirical distribution of $R_{g_q}^Q$ and $R_{g_k}^K$, thereby shrinking the theoretical upper bound U_{g_q, g_k} and narrowing the gap between block-wise attention estimation and the oracle full-attention baseline. We visualize the effect by comparing the relationship between the theoretical bound U_{g_q, g_k} and the actual maximum logit deviation $\|\hat{\ell}_{ij} - \ell_{g_q, g_k}\|$ before (blue) and after (red) applying norm-based ranking in Fig. 2. The improvement of the correlation coefficient R shows that norm-based ranking not only reduces the magnitude of the bound but also enhances its predictive power, making it a more faithful proxy for the true approximation error. Importantly, this process is entirely deterministic and parameter-free, aligning with our training-free design philosophy while providing a principled means to control the approximation error between m and \hat{m} .

3.4. Covariance-Based Compensation

Recalling the logit decomposition. From the token/block logit relation in Eq. (5), we have

$$\hat{\ell}_{ij} - \ell_{g_q, g_k} = \frac{1}{\sqrt{d}} \left(\underbrace{\delta Q_i \cdot \bar{K}_{g_k}}_{(I)} + \underbrace{\bar{Q}_{g_q} \cdot \delta K_j}_{(II)} + \underbrace{\delta Q_i \cdot \delta K_j}_{(III)} \right). \quad (11)$$

By construction $\mathbb{E}_{i \in I(g_q)}[\delta Q_i] = \mathbf{0}$ and $\mathbb{E}_{j \in J(g_k)}[\delta K_j] = \mathbf{0}$, so the *block expectation* of (I) and (II) vanishes, whereas (III) may leave a *systematic bias*:

$$\mathbb{E}_{i,j}[\hat{\ell}_{ij} - \ell_{g_q, g_k}] = \frac{1}{\sqrt{d}} \mathbb{E}_{i,j}[\delta Q_i^\top \delta K_j] \approx \frac{1}{d} \text{tr}(\Sigma_{g_q}^Q \Sigma_{g_k}^K), \quad (12)$$

where $\Sigma_{g_q}^Q = \mathbb{E}_i[\delta Q_i \delta Q_i^\top]$ and $\Sigma_{g_k}^K = \mathbb{E}_j[\delta K_j \delta K_j^\top]$. Equation (12) reveals that even after reducing the variance-like terms via norm-based ranking (*i.e.* tightening U_{g_q, g_k} in Eq. (8)), a *second-order* covariance contribution can still bias the block logits.

Designing the compensation term. Guided by (12), we add a lightweight second-order correction to the block logit:

$$\tilde{\ell}_{g_q, g_k} = \ell_{g_q, g_k} + \beta \Delta_{g_q, g_k}, \Delta_{g_q, g_k} := \frac{1}{d} \text{tr}(\Sigma_{g_q}^Q \Sigma_{g_k}^K), \quad (13)$$

where β is a scalar to balance fidelity and stability (default $\beta=1$). Intuitively, Δ_{g_q, g_k} upweights blocks whose query/key residuals are more correlated, recovering contrast that is lost when using block means alone.

Diagonal (variance) approximation and complexity. Computing $\text{tr}(\Sigma^Q \Sigma^K)$ exactly costs $O(Ld^2)$. In practice, we adopt a diagonal-variance approximation that yields

Algorithm 1 Norm-Rank Attention with Covariance Compensation (Block Approximate Sparse Attention)

Require: Inputs Q, K, V ; block size B ; per-query-block budget κ ; compensation weight β .

- 1: **Query Ranking by Norm:** compute $s_i^Q = \|Q_i\|_2$, obtain permutation π_q by (windowed) sort, and reorder $Q'_i \leftarrow Q_{\pi_q(i)}$
 - 2: **Key Ranking by Norm:** compute $s_j^K = \|K_j\|_2$, obtain π_k , and reorder $K'_j \leftarrow K_{\pi_k(j)}$, $V'_j \leftarrow V_{\pi_k(j)}$
 - 3: **Block Partition:** divide Q', K' into blocks $\{I(g_q)\}_{g_q=1}^{N_q}$ and $\{J(g_k)\}_{g_k=1}^{N_k}$ of size B
 - 4: **Block Statistics:** for each (g_q, g_k) , compute block means $\bar{Q}_{g_q}, \bar{K}_{g_k}$ and covariances $\Sigma_{g_q}^Q, \Sigma_{g_k}^K$
 - 5: **Baseline Logits:** $\ell_{g_q, g_k} = \frac{1}{\sqrt{d}} \bar{Q}_{g_q} \cdot \bar{K}_{g_k}$
 - 6: **Covariance Compensation:** compute $\hat{\Delta}_{g_q, g_k}$ in Eq. (14)
 - 7: **Compensated Block Logits:** $\ell'_{g_q, g_k} \leftarrow \ell_{g_q, g_k} + \beta \hat{\Delta}_{g_q, g_k}$
 - 8: **for** each query block $g_q = 1, \dots, N_q$ **do**
 - 9: $m'_{g_q, \cdot} \leftarrow \text{softmax}(\{\ell'_{g_q, g_k}\}_{g_k})$
 - 10: select top- κ key blocks by $m'_{g_q, \cdot}$; set $M_{g_q, g_k} = 1$ if selected, else 0
 - 11: **end for**
 - 12: **Block Sparse Attention Computation:** execute block-sparse attention on Q', K', V' over $\{(g_q, g_k) : M_{g_q, g_k} = 1\}$ using Triton kernels; remap outputs to the original order via π_q^{-1}
 - 13: **return** Sparse attention outputs
-

three additive terms:

$$\Delta_{g_q, g_k} \approx \frac{1}{d} \sum_{t=1}^d \left(\text{Var}[Q_t]_{g_q} \bar{K}_{g_k, t}^2 + \text{Var}[K_t]_{g_k} \bar{Q}_{g_q, t}^2 + \text{Var}[Q_t]_{g_q} \text{Var}[K_t]_{g_k} \right). \quad (14)$$

It only requires blockwise first/second moments (computed alongside \bar{Q}, \bar{K}), adds $O((N_q + N_k)d)$ extra work per layer, and keeps the overall complexity $O(Ld)$.

Summary. Norm-based ranking primarily *reduces variance* (tightening U_{g_q, g_k}), while covariance-based compensation *removes residual bias* predicted by (11). The two are complementary: together they narrow the gap between the practical downsampled distribution m and the oracle \hat{m} without any training or dense-map construction. Finally, we summarize the Block Approximate Sparse Attention framework and provide pseudo-code in Algorithm 1.

Table 2. Comparison of different attention methods on the LongBench benchmark truncated to a 16K context length, implemented with LLaDA1.5 and UltraLLaDA. AVG is an aggregated question-count-weighted average score.

Method	Single-Doc QA				Multi-Doc QA				Summarization				Few-shot Learning				Synthetic			Code		AVG
	<i>NrrVQA</i>	<i>Qasper</i>	<i>MF-en</i>	<i>MF-zh</i>	<i>HPQA</i>	<i>2WikiMQA</i>	<i>MuSiQue</i>	<i>DuReader</i>	<i>GovReport</i>	<i>QMSum</i>	<i>MultiNews</i>	<i>VCSum</i>	<i>TREC</i>	<i>TriviaQA</i>	<i>SAMSum</i>	<i>LSHT</i>	<i>PassCount</i>	<i>PassRe-en</i>	<i>PassRe-zh</i>	<i>LCC</i>	<i>RB-p</i>	
LLaDA1.5	4.1	20.4	21.8	20.8	6.3	8.1	3.4	10.5	17.3	5.4	14.3	6.7	73.5	63.6	32.2	21.5	1.9	29.5	70.9	68.0	60.6	31.5
+XAtt	4.3	20.3	21.5	19.9	7.5	7.9	3.5	10.8	16.8	5.8	14.2	7.5	61.5	61.5	28.7	19.3	1.9	27.7	56.8	61.9	55.0	28.8
+Ours	4.9	20.4	21.8	20.1	6.3	8.0	3.7	11.2	17.4	5.4	14.4	6.7	71.0	60.1	33.6	22.3	2.1	28.4	68.2	67.9	60.8	31.3
UltraLLaDA	12.1	14.5	27.4	19.9	13.4	11.0	9.7	20.4	20.8	7.8	14.7	7.5	79.5	92.0	36.2	40.5	0.7	81.3	72.9	66.2	56.9	37.2
+XAtt	4.1	13.9	25.2	20.1	6.2	6.8	5.2	12.9	19.9	7.0	16.0	7.4	75.0	85.2	33.3	28.5	2.1	81.4	64.6	64.5	63.5	34.9
+Ours	13.3	13.6	27.9	20.3	13.8	9.8	8.7	12.6	20.8	7.9	12.7	8.3	75.5	90.9	35.5	34.4	1.3	82.3	70.9	69.0	63.1	37.2

Table 3. Comparison of different attention methods on the RULER benchmark across context lengths from 4K to 32K, using LLaDA1.5 and UltraLLaDA as base models. Evaluated categories include: Retrieval (Needle-in-a-Haystack, NIAH), Aggregation (frequent word extraction, AGG), Question Answering (QA), and Multi-hop Tracing (variable tracking, VT). AVG denotes a question-count-weighted average score across all categories. “-” indicates failure.

Model	4K					8K				
	NIAH	AGG	QA	VT	AVG	NIAH	AGG	QA	VT	AVG
LLaDA1.5	99.25	47.78	88.5	100	89.74	51.56	41.6	48.02	61.6	50.25
LLaDA1.5+XAtt	74.66	26.55	61.00	3.00	59.64	39.53	33.21	35.5	0.4	34.93
LLaDA1.5+Ours	98.16	41.20	85.5	99.4	87.54	50.28	58.23	48.1	59.4	51.85
UltraLLaDA	97.31	66.69	68.50	100	88.37	98.28	55.29	62.00	100	86.22
UltraLLaDA+XAtt	95.12	49.61	70.50	57.40	81.43	86.97	36.30	62.00	24.20	70.50
UltraLLaDA+Ours	98.16	67.78	75.00	100	90.06	98.5	57.65	68.50	100	87.71

Model	16K					32K				
	NIAH	AGG	QA	VT	AVG	NIAH	AGG	QA	VT	AVG
LLaDA1.5	8.56	11.19	46.5	20.6	15.73	-	-	-	-	-
LLaDA1.5+XAtt	15.16	15.89	37.00	0.6	17.51	-	-	-	-	-
LLaDA1.5+Ours	16.5	18.06	74.00	30.00	26.62	-	-	-	-	-
UltraLLaDA	93.00	43.12	39.50	98.40	77.51	92.78	29.29	29.00	98.40	73.63
UltraLLaDA+XAtt	75.09	35.37	40.00	7.40	58.38	74.94	30.19	15.50	1.80	53.28
UltraLLaDA+Ours	94.62	44.89	53.00	99.40	80.93	90.97	27.85	32.00	100	72.88

4. Experiments

4.1. Experimental Settings

Baselines and Platforms We evaluate our block-sparse attention framework across three distinct domains. (1) For natural language tasks, we employ LLaDA1.5 [66] and UltraLLaDA [18]. (2) In the multi-modal understanding domain, we utilize LLaDA-V [54]. (3) Finally, for video generation, we use the Wan2.1-T2V-14B [40]. Our dense attention baseline is implemented using FLASHATTENTION-2 [8] within the FLASHINFER [53] framework. We utilize SVG2 [50] as a strong baseline for video generation. All experiments are conducted on the NVIDIA A100 (80GB) GPU platform using PyTorch. We optimize kernel performance via Triton with a block size of 128 and use greedy decoding. For ULTRALLADA, LLADA1.5, and LLADA-V, we set the sparsity over 50% and integrate the FAST-DLLM [42] for fast evaluation.

Datasets and Implementation We evaluate our model across three domains: natural language understanding, vision understanding, and video generation. For Natural Language Understanding, we use the RULER dataset [19] to test long-context reasoning with controllable sequence lengths and task complexities, and the LongBench benchmark [1] for real-world long-context evaluation. Second, we adopt ChartQA [31], DocVQA [32], InfoVQA [33], RealworldQA [44], MMMU [56], and MMMU-Pro [57] for image-language tasks. Next, for multi-image and video understanding, we evaluate on Video-MME [12], MLVU-dev [65], and MuirBench [41], which stress-test sparse attention under long visual contexts. Notably, Video-MME includes 900 videos (totaling 254 hours) and serves as a large-scale benchmark for multi-modal video comprehension. Finally, in video generation tasks, we use 96 text prompts from VBench [20] to generate videos, comparing with a full-attention baseline to assess generation.

Table 4. Comparison of different methods on LLaDA-V in video understanding tasks. All metrics are reported as percentages. Higher is better. AVG is the average score across all datasets.

Model	VideoMME	MLVU-dev	MuirBench
LLaDA-V	56.07	59.61	48.12
LLaDA-V+Flex	48.22	47.91	34.35
LLaDA-V+XAtt	55.63	53.84	46.54
LLaDA-V+Ours	56.56	59.71	47.69

4.2. Performance Evaluation

Performance on Ultra-Long NLP Tasks. Our method effectively improves long-context performance across both LLaDA-1.5 and UltraLLaDA models, as shown in Tab. 3. UltraLLaDA+Ours achieves the best overall results, demonstrating that our attention mechanism effectively preserves task-critical information while enabling efficient computation. As shown in Tab. 2, our method demonstrates strong *task-agnostic* effectiveness: it preserves or slightly enhances performance across all categories without task-specific tuning. This contrasts with XAttention, whose fixed sparsity pattern leads to inconsistent gains and notable drops in NarrativeQA and PassRe-zh tasks. The results suggest that our sorting and compensation scheme generalizes well beyond controlled benchmarks to diverse, practical long-context scenarios.

Performance on Multimodal Understanding On the video understanding benchmarks (Tab. 4), our method achieves consistent gains over the LLaDA-V baseline across all datasets, achieving slightly better results on VideoMME and MLVU-dev.

In Tab. 6, we show the result on general image understanding tasks. LLaDA-V+Ours matches or exceeds the strong LLaDA-V baseline across diverse tasks—from chart and document understanding to complex multi-modal QA—while significantly outperforming sparsity-based alternatives like Flex and XAtt. Notably, our approach achieves the highest overall average, demonstrating that our prior-free sparse pattern preserves critical visual-semantic information without sacrificing efficiency.

Performance on Video Generation We conduct experiments on the VBench using the Wan2.1 model, with a 10-step full-attention warmup to ensure stable generation. The generated videos are produced using 50 denoising steps, resulting in an input sequence of approximately 75K tokens in context length. As shown in Tab. 5, our approach achieves significantly higher visual fidelity than SVG2, which is a dedicated video generation accelerator, across all metrics—especially at 60% and 50% sparsity. It improves PSNR by over 2.5 dB and reduces LPIPS by 35%. Qualitatively, as illustrated in Fig. 3, our method generates videos with consistent object appearance and accurate fine-grained details, closely matching the full-attention baseline while maintaining sparsity and efficiency.

Table 5. Quantitative results of applying Sparse Attention methods to the Wan2.1 model on the VBench benchmark, using a 10-step full-attention warmup. Higher (\uparrow) yields better fidelity at the cost of slightly reduced sparsity (higher density).

Methods	PSNR (\uparrow)	SSIM (\uparrow)	MS_SSIM (\uparrow)	LPIPS (\downarrow)
SVG2	21.51	0.762	0.832	0.173
Ours(60%)	22.34	0.782	0.865	0.163
Ours(50%)	24.08	0.833	0.906	0.112

4.3. Ablation Study

Attention Acceleration We measure operator-level speedup over baseline across sequence lengths from 16K to 256K tokens. As shown in Fig. 4, our method variants achieve substantial acceleration, with “Ours (Sort)” delivering up to **6.95** \times speedup at 256K significantly outperforming both Flex (4.56 \times) and XAttn-8 (3.5 \times). To balance fidelity and efficiency, we apply covariance compensation only in the first and last layers, where attention patterns are most sensitive and diverse. This selective use yields “Ours (Sort+Cov)”, which retains a strong 5.70 \times speedup at 256K while improving output quality.

Norm-based Sort Analysis In Tab. 7, we present the performance of various norm-based sorting strategies on Ruler-4K under different sparsity levels. Notably, jointly sorting queries and keys (SortQ+SortK) further improves performance at higher sparsity levels, suggesting that aligning both query and key orderings enhances the effectiveness of block-sparse attention. These results validate that norm-based reordering—particularly of keys—effectively concentrates salient information into fewer blocks, enabling sparse attention to retain more task-relevant signals.

5. Related Work

Diffusion Language Models Diffusion-based generative models, originally developed for continuous data like images [11], have recently been adapted to text generation through continuous [4, 10, 15–17, 25, 26, 28, 30, 36, 37, 43, 49, 52, 60, 61] and discrete [5, 14, 22, 35, 38, 51, 63, 64] variants. Unlike autoregressive models that generate tokens sequentially, Diffusion Language Models (DLMs) denoise an entire sequence in parallel, offering the potential for faster decoding. Recent works such as UltraLLaDA [18], LongLLaDA [27] and LLaDA-V [54] demonstrate that DLMs can achieve competitive performance on language and multi-modal tasks. However, the quadratic complexity of full-attention over long denoising sequences remains a major bottleneck, especially in multi-modal or document-level applications.

Sparse Attention To mitigate the quadratic complexity of self-attention, several sparse attention mechanisms have been proposed [29, 45, 55, 59]. Early approaches em-

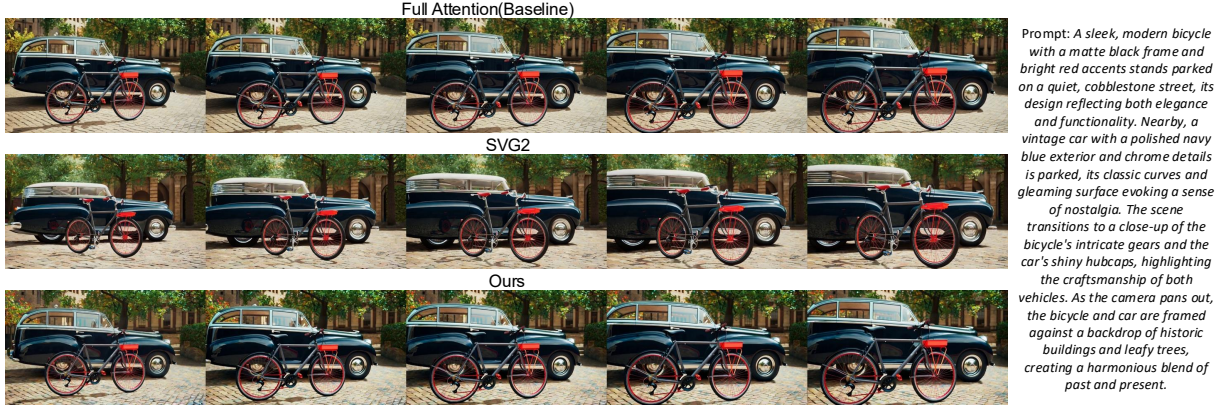


Figure 3. Qualitative comparison of video generation results on the VBench benchmark dataset. Rows show frames from videos generated using: (1) Full Attention (baseline), (2) SVG2, (3) Ours. Our method achieves high visual fidelity to the full attention baseline.

Table 6. Comparison of different methods on LLaDA-V in various visual understanding tasks. All metrics are reported as percentages. Higher is better. AVG is the average score across all datasets.

Model	ChartQA	DocVQA(val)	InfoVQA(val)	RealworldQA	MMMU(val)	MMMU(ProVision)	AVG
LLaDA-V	77.8	83.48	<u>65.02</u>	63.01	48.67	18.60	<u>59.43</u>
LLaDA-V + Flex	54.0	30.29	26.75	48.76	44.91	14.51	36.54
LLaDA-V + XAtt	72.56	82.31	62.88	63.14	44.44	16.18	56.92
LLaDA-V + Ours	<u>77.72</u>	<u>82.89</u>	65.26	64.84	<u>48.32</u>	<u>17.92</u>	59.49

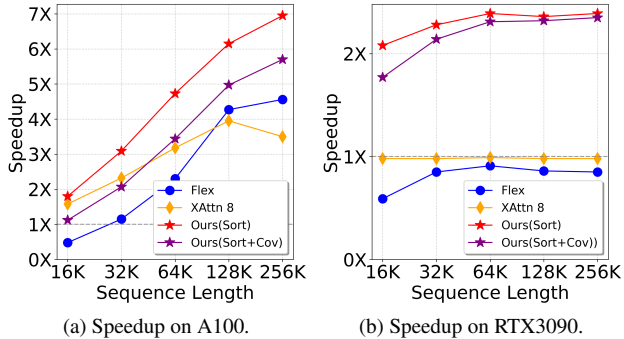


Figure 4. Operator-level speedup over flash-attention baseline. Our method variants consistently outperform prior approaches across various context-length and devices.

Table 7. Performance on Ruler-4K under different norm sort strategies and sparsity settings.

Sparsity	90%	70%	50%
Baseline	22.34	52.91	81.08
SortQ	24.07	55.66	82.64
SortK	27.13	60.56	87.25
SortQ+SortK	26.98	61.66	88.27

ploy fixed sparsity patterns, such as local windows or strided blocks [2, 58], which effectively reduce computational cost but often struggle to capture long-range dependencies crucial for reasoning and understanding global context [6, 24]. More recent methods adopt adaptive or data-driven sparsity. H2O [62] and TOVA [34] discard tokens

based on query patterns. SeerAttention [13] proposes a lightweight learnable module for sparse pattern selection, while XAttention [48] introduces an anti-diagonal block selection strategy that efficiently models long-range interactions. StreamingLLM [46] observes that certain early tokens act as “sinks” that stabilize attention in streaming LMs.

6. Conclusion and Limitation

Conclusion. In this work, we proposed a block-sparse attention framework for diffusion language models, introducing a pre-downsampled block-sparse mechanism that evaluates block informativeness before attention computation. Through norm-based ranking and covariance-compensated correction, our method effectively reduces approximation error and achieves substantial acceleration while maintaining near full-attention fidelity across diverse modalities and tasks. Extensive experiments demonstrate up to 6.95× speedup on 128K-sequence inference with minimal accuracy degradation, validating the scalability and generalization of our approach in ultra-long context modeling.

Limitations. Despite these promising results, several limitations remain. First, our current design focuses on diffusion-based models; extending the proposed mechanism to AR models may reveal additional challenges in maintaining causal masking. Besides, the current covariance-compensated correction involves partial covariance estimation to improve fidelity. There is potential for further acceleration through triton or low-rank approximations.

7. Acknowledgements

This work was supported in part by the Research Grants Council under the Areas of Excellence scheme grant AoE/E-601/22-R.

References

- [1] Yushi Bai, Xin Lv, Jiajie Zhang, Hongchang Lyu, Jiankai Tang, Zhidian Huang, Zhengxiao Du, Xiao Liu, Aohan Zeng, Lei Hou, Yuxiao Dong, Jie Tang, and Juanzi Li. Longbench: A bilingual, multitask benchmark for long context understanding. *arXiv preprint arXiv:2308.14508*, 2023. 6
- [2] Iz Beltagy, Matthew E. Peters, and Arman Cohan. Longformer: The long-document transformer. *arXiv:2004.05150*, 2020. 8
- [3] Stephen Boyd and Lieven Vandenbergh. *Convex Optimization*. Cambridge University Press, Cambridge, UK, 2004. 3
- [4] Ting Chen, Ruixiang Zhang, and Geoffrey Hinton. Analog bits: Generating discrete data using diffusion models with self-conditioning. *arXiv preprint arXiv:2208.04202*, 2022. 7
- [5] Zixiang Chen, Huizhuo Yuan, Yongqian Li, Yiwen Kou, Junkai Zhang, and Quanquan Gu. Fast sampling via de-randomization for discrete diffusion models. *arXiv preprint arXiv:2312.09193*, 2023. 7
- [6] Rewon Child, Scott Gray, Alec Radford, and Ilya Sutskever. Generating long sequences with sparse transformers, 2019. 8
- [7] Krzysztof Choromanski, Valerii Likhoshesterov, David Dohan, Xingyou Song, Andreea Gane, Tamas Sarlos, Peter Hawkins, Jared Davis, Afroz Mohiuddin, Lukasz Kaiser, David Belanger, Lucy Colwell, and Adrian Weller. Rethinking attention with performers, 2022. 3
- [8] Tri Dao. FlashAttention-2: Faster attention with better parallelism and work partitioning, 2023. 2, 6
- [9] Tri Dao, Daniel Y. Fu, Stefano Ermon, Atri Rudra, and Christopher Ré. Flashattention: Fast and memory-efficient exact attention with io-awareness, 2022. 3
- [10] Sander Dieleman, Laurent Sartran, Arman Roshannai, Nikolay Savinov, Yaroslav Ganin, Pierre H Richemond, Arnaud Doucet, Robin Strudel, Chris Dyer, Conor Durkan, et al. Continuous diffusion for categorical data. *arXiv preprint arXiv:2211.15089*, 2022. 7
- [11] Patrick Esser, Sumith Kulal, Andreas Blattmann, Rahim Entezari, Jonas Müller, Harry Saini, Yam Levi, Dominik Lorenz, Axel Sauer, Frederic Boesel, Dustin Podell, Tim Dockhorn, Zion English, Kyle Lacey, Alex Goodwin, Yan-nik Marek, and Robin Rombach. Scaling rectified flow transformers for high-resolution image synthesis, 2024. 7
- [12] Chaoyou Fu, Yuhan Dai, Yondong Luo, Lei Li, Shuhuai Ren, Renrui Zhang, Zihan Wang, Chenyu Zhou, Yunhang Shen, Mengdan Zhang, et al. Video-mme: The first-ever comprehensive evaluation benchmark of multi-modal llms in video analysis. *arXiv preprint arXiv:2405.21075*, 2024. 6
- [13] Yizhao Gao, Zhichen Zeng, Dayou Du, Shijie Cao, Peiyuan Zhou, Jiaying Qi, Junjie Lai, Hayden Kwok-Hay So, Ting Cao, Fan Yang, and Mao Yang. Seerattention: Learning intrinsic sparse attention in your llms, 2025. 1, 2, 4, 8
- [14] Itai Gat, Tal Remez, Neta Shaul, Felix Kreuk, Ricky TQ Chen, Gabriel Synnaeve, Yossi Adi, and Yaron Lipman. Discrete flow matching. *arXiv preprint arXiv:2407.15595*, 2024. 7
- [15] Shansan Gong, Mukai Li, Jiangtao Feng, Zhiyong Wu, and LingPeng Kong. Diffuseq: Sequence to sequence text generation with diffusion models. *arXiv preprint arXiv:2210.08933*, 2022. 7
- [16] Alex Graves, Rupesh Kumar Srivastava, Timothy Atkinson, and Faustino Gomez. Bayesian flow networks. *arXiv preprint arXiv:2308.07037*, 2023.
- [17] Xiaochuang Han, Sachin Kumar, and Yulia Tsvetkov. Ssd-lm: Semi-autoregressive simplex-based diffusion language model for text generation and modular control. *arXiv preprint arXiv:2210.17432*, 2022. 7
- [18] Guangxin He, Shen Nie, Fengqi Zhu, Yuankang Zhao, Tianyi Bai, Ran Yan, Jie Fu, Chongxuan Li, and Binhang Yuan. Ultrallada: Scaling the context length to 128k for diffusion large language models, 2025. 6, 7
- [19] Cheng-Ping Hsieh, Simeng Sun, Samuel Kriman, Shantanu Acharya, Dima Rekesh, Fei Jia, Yang Zhang, and Boris Ginsburg. Ruler: What’s the real context size of your long-context language models? *arXiv preprint arXiv:2404.06654*, 2024. 6
- [20] Ziqi Huang, Yinan He, Jiashuo Yu, Fan Zhang, Chenyang Si, Yuming Jiang, Yuanhan Zhang, Tianxing Wu, Qingyang Jin, Nattapol Chanpaisit, Yaohui Wang, Xinyuan Chen, Limin Wang, Dahua Lin, Yu Qiao, and Ziwei Liu. VBench: Comprehensive benchmark suite for video generative models. In *Proceedings of the IEEE/CVF Conference on Computer Vision and Pattern Recognition*, 2024. 6
- [21] Huiqiang Jiang, Yucheng Li, Chengruidong Zhang, Qianhui Wu, Xufang Luo, Surin Ahn, Zhenhua Han, Amir H. Abdi, Dongsheng Li, Chin-Yew Lin, Yuqing Yang, and Lili Qiu. Minference 1.0: Accelerating pre-filling for long-context llms via dynamic sparse attention, 2024. 1, 2
- [22] Ouail Kitouni, Niklas Nolte, James Hensman, and Bhaskar Mitra. Disk: A diffusion model for structured knowledge. *arXiv preprint arXiv:2312.05253*, 2023. 7
- [23] Xunhao Lai, Jianqiao Lu, Yao Luo, Yiyuan Ma, and Xun Zhou. Flexprefill: A context-aware sparse attention mechanism for efficient long-sequence inference, 2025. 1, 2
- [24] Yaniv Leviathan, Matan Kalman, and Yossi Matias. Selective attention improves transformer, 2024. 8
- [25] Xiang Li, John Thickstun, Ishaan Gulrajani, Percy S Liang, and Tatsunori B Hashimoto. Diffusion-lm improves controllable text generation. *Advances in Neural Information Processing Systems*, 35:4328–4343, 2022. 7
- [26] Zhenghao Lin, Yeyun Gong, Yelong Shen, Tong Wu, Zhihao Fan, Chen Lin, Nan Duan, and Weizhu Chen. Text generation with diffusion language models: A pre-training approach with continuous paragraph denoise. In *International Conference on Machine Learning*, pages 21051–21064. PMLR, 2023. 7

- [27] Xiaoran Liu, Zhigeng Liu, Zengfeng Huang, Qipeng Guo, Ziwei He, and Xipeng Qiu. Longllada: Unlocking long context capabilities in diffusion llms, 2025. 7
- [28] Aaron Lou and Stefano Ermon. Reflected diffusion models, 2023. 7
- [29] Enzhe Lu, Zhejun Jiang, Jingyuan Liu, Yulun Du, Tao Jiang, Chao Hong, Shaowei Liu, Weiran He, Enming Yuan, Yuzhi Wang, Zhiqi Huang, Huan Yuan, Suting Xu, Xinran Xu, Guokun Lai, Yanru Chen, Huabin Zheng, Junjie Yan, Jianlin Su, Yuxin Wu, Neo Y. Zhang, Zhilin Yang, Xinyu Zhou, Mingxing Zhang, and Jiezhong Qiu. Moba: Mixture of block attention for long-context llms, 2025. 7
- [30] Rabeeh Karimi Mahabadi, Hamish Ivison, Jaesung Tae, James Henderson, Iz Beltagy, Matthew E. Peters, and Arman Cohan. Tess: Text-to-text self-conditioned simplex diffusion, 2024. 7
- [31] Ahmed Masry, Do Xuan Long, Jia Qing Tan, Shafiq Joty, and Enamul Hoque. Chartqa: A benchmark for question answering about charts with visual and logical reasoning. *arXiv preprint arXiv:2203.10244*, 2022. 6
- [32] Minesh Mathew, Dimosthenis Karatzas, and CV Jawahar. Docvqa: A dataset for vqa on document images. In *Proceedings of the IEEE/CVF winter conference on applications of computer vision*, pages 2200–2209, 2021. 6
- [33] Minesh Mathew, Viraj Bagal, Rubèn Tito, Dimosthenis Karatzas, Ernest Valveny, and CV Jawahar. Infographicvqa. In *Proceedings of the IEEE/CVF Winter Conference on Applications of Computer Vision*, pages 1697–1706, 2022. 6
- [34] Matanel Oren, Michael Hassid, Nir Yarden, Yossi Adi, and Roy Schwartz. Transformers are multi-state rnns, 2024. 8
- [35] Machel Reid, Vincent J. Hellendoorn, and Graham Neubig. Diffuser: Discrete diffusion via edit-based reconstruction, 2022. 7
- [36] Pierre H. Richemond, Sander Dieleman, and Arnaud Doucet. Categorical sdes with simplex diffusion, 2022. 7
- [37] Robin Strudel, Corentin Tallec, Florent Althé, Yilun Du, Yaroslav Ganin, Arthur Mensch, Will Grathwohl, Nikolay Savinov, Sander Dieleman, Laurent Sifre, et al. Self-conditioned embedding diffusion for text generation. *arXiv preprint arXiv:2211.04236*, 2022. 7
- [38] Haoran Sun, Lijun Yu, Bo Dai, Dale Schuurmans, and Hanjun Dai. Score-based continuous-time discrete diffusion models. *arXiv preprint arXiv:2211.16750*, 2022. 7
- [39] Philippe Tillet, H. T. Kung, and David Cox. Triton: an intermediate language and compiler for tiled neural network computations. In *Proceedings of the 3rd ACM SIGPLAN International Workshop on Machine Learning and Programming Languages*, page 10–19, New York, NY, USA, 2019. Association for Computing Machinery. 3
- [40] Team Wan, Ang Wang, and Baole Ai et al. Wan: Open and advanced large-scale video generative models, 2025. 6
- [41] Fei Wang, Xingyu Fu, James Y Huang, Zekun Li, Qin Liu, Xiaogeng Liu, Mingyu Derek Ma, Nan Xu, Wenxuan Zhou, Kai Zhang, et al. Muirbench: A comprehensive benchmark for robust multi-image understanding. *arXiv preprint arXiv:2406.09411*, 2024. 6
- [42] Chengyue Wu, Hao Zhang, Shuchen Xue, Zhijian Liu, Shizhe Diao, Ligeng Zhu, Ping Luo, Song Han, and Enze Xie. Fast-dllm: Training-free acceleration of diffusion llm by enabling kv cache and parallel decoding, 2025. 6
- [43] Tong Wu, Zhihao Fan, Xiao Liu, Yeyun Gong, Yelong Shen, Jian Jiao, Hai-Tao Zheng, Juntao Li, Zhongyu Wei, Jian Guo, Nan Duan, and Weizhu Chen. Ar-diffusion: Auto-regressive diffusion model for text generation, 2023. 7
- [44] x.ai. Grok-1.5 vision preview. 2024. <https://x.ai/news/grok-1.5v/>. 6
- [45] Haocheng Xi, Shuo Yang, Yilong Zhao, Chenfeng Xu, Muyang Li, Xiuyu Li, Yujun Lin, Han Cai, Jintao Zhang, Dacheng Li, Jianfei Chen, Ion Stoica, Kurt Keutzer, and Song Han. Sparse videogen: Accelerating video diffusion transformers with spatial-temporal sparsity, 2025. 7
- [46] Guangxuan Xiao, Yuandong Tian, Beidi Chen, Song Han, and Mike Lewis. Efficient streaming language models with attention sinks, 2024. 8
- [47] Guangxuan Xiao, Yuandong Tian, Beidi Chen, Song Han, and Mike Lewis. Efficient streaming language models with attention sinks. In *ICLR*, 2024. 1
- [48] Ruyi Xu, Guangxuan Xiao, Haofeng Huang, Junxian Guo, and Song Han. Xattention: Block sparse attention with anti-diagonal scoring, 2025. 1, 2, 8
- [49] Kaiwen Xue, Yuhao Zhou, Shen Nie, Xu Min, Xiaolu Zhang, Jun Zhou, and Chongxuan Li. Unifying bayesian flow networks and diffusion models through stochastic differential equations. *arXiv preprint arXiv:2404.15766*, 2024. 7
- [50] Shuo Yang, Haocheng Xi, Yilong Zhao, Muyang Li, Jintao Zhang, Han Cai, Yujun Lin, Xiuyu Li, Chenfeng Xu, Kelly Peng, Jianfei Chen, Song Han, Kurt Keutzer, and Ion Stoica. Sparse videogen2: Accelerate video generation with sparse attention via semantic-aware permutation, 2025. 6
- [51] Jiasheng Ye, Zaixiang Zheng, Yu Bao, Lihua Qian, and Quanquan Gu. Diffusion language models can perform many tasks with scaling and instruction-finetuning. *arXiv preprint arXiv:2308.12219*, 2023. 7
- [52] Jiasheng Ye, Zaixiang Zheng, Yu Bao, Lihua Qian, and Mingxuan Wang. Dinoiser: Diffused conditional sequence learning by manipulating noises. *arXiv preprint arXiv:2302.10025*, 2023. 7
- [53] Zihao Ye, Ruihang Lai, Roy Lu, Chien-Yu Lin, Size Zheng, Lequn Chen, Tianqi Chen, and Luis Ceze. Cascade inference: Memory bandwidth efficient shared prefix batch decoding. <https://flashinfer.ai/2024/01/08/cascade-inference.html>, 2024. Accessed on 2024-02-01. 6
- [54] Zebin You, Shen Nie, Xiaolu Zhang, Jun Hu, Jun Zhou, Zhiwu Lu, Ji-Rong Wen, and Chongxuan Li. Llada-v: Large language diffusion models with visual instruction tuning, 2025. 6, 7
- [55] Jingyang Yuan, Huazuo Gao, Damai Dai, Junyu Luo, Liang Zhao, Zhengyan Zhang, Zhenda Xie, Y. X. Wei, Lean Wang, Zhiping Xiao, Yuqing Wang, Chong Ruan, Ming Zhang, Wenfeng Liang, and Wangding Zeng. Native sparse attention: Hardware-aligned and natively trainable sparse attention, 2025. 7

- [56] Xiang Yue, Yuansheng Ni, Kai Zhang, Tianyu Zheng, Ruoqi Liu, Ge Zhang, Samuel Stevens, Dongfu Jiang, Weiming Ren, Yuxuan Sun, et al. Mmmu: A massive multi-discipline multimodal understanding and reasoning benchmark for expert agi. In *Proceedings of the IEEE/CVF Conference on Computer Vision and Pattern Recognition*, pages 9556–9567, 2024. [6](#)
- [57] Xiang Yue, Tianyu Zheng, Yuansheng Ni, Yubo Wang, Kai Zhang, Shengbang Tong, Yuxuan Sun, Botao Yu, Ge Zhang, Huan Sun, et al. Mmmu-pro: A more robust multi-discipline multimodal understanding benchmark. *arXiv preprint arXiv:2409.02813*, 2024. [6](#)
- [58] Manzil Zaheer, Guru Guruganesh, Kumar Avinava Dubey, Joshua Ainslie, Chris Alberti, Santiago Ontanon, Philip Pham, Anirudh Ravula, Qifan Wang, Li Yang, et al. Big bird: Transformers for longer sequences. *Advances in Neural Information Processing Systems*, 33, 2020. [8](#)
- [59] Peiyuan Zhang, Yongqi Chen, Runlong Su, Hangliang Ding, Ion Stoica, Zhenghong Liu, and Hao Zhang. Fast video generation with sliding tile attention, 2025. [7](#)
- [60] Ruixiang Zhang, Shuangfei Zhai, Yizhe Zhang, James Thornton, Zijing Ou, Joshua Susskind, and Navdeep Jaitly. Target concrete score matching: A holistic framework for discrete diffusion. *arXiv preprint arXiv:2504.16431*, 2025. [7](#)
- [61] Yizhe Zhang, Jiatao Gu, Zhuofeng Wu, Shuangfei Zhai, Joshua Susskind, and Navdeep Jaitly. Planner: Generating diversified paragraph via latent language diffusion model. *Advances in Neural Information Processing Systems*, 36: 80178–80190, 2023. [7](#)
- [62] Zhenyu Zhang, Ying Sheng, Tianyi Zhou, Tianlong Chen, Lianmin Zheng, Ruisi Cai, Zhao Song, Yuandong Tian, Christopher Ré, Clark Barrett, Zhangyang Wang, and Beidi Chen. H₂o: Heavy-hitter oracle for efficient generative inference of large language models, 2023. [8](#)
- [63] Kaiwen Zheng, Yongxin Chen, Hanzi Mao, Ming-Yu Liu, Jun Zhu, and Qinsheng Zhang. Masked diffusion models are secretly time-agnostic masked models and exploit inaccurate categorical sampling, 2024. [7](#)
- [64] Lin Zheng, Jianbo Yuan, Lei Yu, and Lingpeng Kong. A reparameterized discrete diffusion model for text generation. *ArXiv*, abs/2302.05737, 2023. [7](#)
- [65] Junjie Zhou, Yan Shu, Bo Zhao, Boya Wu, Shitao Xiao, Xi Yang, Yongping Xiong, Bo Zhang, Tiejun Huang, and Zheng Liu. Mlvu: A comprehensive benchmark for multi-task long video understanding. *arXiv preprint arXiv:2406.04264*, 2024. [6](#)
- [66] Fengqi Zhu, Rongzhen Wang, Shen Nie, Xiaolu Zhang, Chunwei Wu, Jun Hu, Jun Zhou, Jianfei Chen, Yankai Lin, Ji-Rong Wen, and Chongxuan Li. Llada 1.5: Variance-reduced preference optimization for large language diffusion models, 2025. [6](#)